Advances in Concrete Construction, *Vol. 9, No. 6 (2020) 537-545*
DOI: https://doi.org/10.12989/acc.2020.9.6.537

A new geopolymeric grout blended completely weathered granite with blast-furnace slag

Jian Zhang[a], Shucai Li[b], Zhaofeng Li*, Hengtian Li[c], Junqi Du[d], Yifan Gao[e], Chao Liu[f], Yanhai Qi[g] and Wenlong Wang[h]

Geotechnical and Structural Engineering Research Center, Shandong University, Jinan, Shandong, 250061, China

(*Received April 12, 2019, Revised May 12, 2020, Accepted May 19, 2020*)

Abstract. In order to reduce the usage of cement slurry in grouting engineering and consume the tunnel excavation waste soil, a new geopolymeric grouting material (GGM) was prepared by combine completely weathered granite (CWG) and blast-furnace slag (BFS), which can be applied to in-situ grouting treatment of completely weathered granite strata. The results showed CWG could participate in the geopolymerization process, and GGM slurry has the characteristics of short setting time, high flowability, low viscosity, high stone rate and high mechanical strength, and a design method of grouting pressure based on viscosity evolution was proposed. By adjusted the content of completely weathered granite and alkali activator concentration, the setting time of GGM were ranged from 5 to 30 minutes, the flowability was more than 23.5 cm, the stone rate was higher than 90%, the compressive strength of 28 days were 7.8-16.9 MPa, the porosity were below 30%. This provides a novel grouting treatment and utilizing excavated soil of tunnels in the similar strata.

Keywords: completely weathered granite; blast-furnace slag; geopolymer; grouting material; flowability; compressive strength; microstructure

1. Introduction

As an effective mean to improve the physical and mechanical properties of rock and soil, grouting has been widely used in underground engineering maintenance, disaster management and other construction fields (Li *et al*. 2016, Hong 2017), and cement slurry is one of the most commonly used grouting materials at present (Yongcheng Zhang 2012). Nevertheless, the ordinary Portland cement industrial discharged about 7% of the total CO_2 emissions of the world in 2017 (Chen *et al*. 2010, Schneider *et al*. 2011), which doesn't meet the development needs of green ecological engineering construction. On the other hand, the large-scale use of cement-based grout in underground engineering construction is too expansive, and increased economic burden on enterprises. It is urgent to develop a green environmental grouting material, so as to realize the environment-friendly and low cost construction of underground engineering.

Geopolymer is a kind of inorganic polymer with a three-dimensional network structure, which is mainly prepared by alumino-silicate raw materials (Davidovits 1991, Duxson 2007). Since the concept of geopolymer proposed by Joseph Davidovits firstly, it has attracted wide attention because of its high mechanical strength, short setting time, high corrosion resistance and low carbon emission (Schneider *et al*. 2011, Mehta and Siddique 2016, Ng *et al*. 2018). With the increasing scarcity of natural resources and the urgent need of global environmental protection, a large number of industrial wastes such as fly ash, blast-furnace slag, agricultural waste and municipal refuse had been studied to prepare geopolymer materials (Jindal *et al*. 2017, Mohamed *et al*. 2017, Tchadjie and Ekolu 2018, Kurtoğlu *et al*. 2018).

Geopolymer has great economic and social benefits for converting waste into high value-added products. Puertas *et al*. prepared fly ash-blast-furnace slag geopolymer and studied the effect of the relative content of fly ash and blast furnace slag, alkali activator concentration and other factors on the geopolymer (Puertas and Fernández-Jiménez 2004), Ping *et al*. (2016) prepared new geopolymer through fly ash and iron tailings, and analyzed the slurry properties, mechanical properties and micro-structure systematically, El-Naggar *et al*. (2017) prepared geopolymer by combined waste glass with metakaolin, and tested the mechanical

*Corresponding author, Ph.D.
E-mail: lizf@sdu.edu.cn
[a]Ph.D. Student
E-mail: zhjian1@126.com
[b]Professor
E-mail: lishucai@sdu.edu.cn
[c]MSc Student
E-mail: liht@mail.sdu.edu.cn
[d]MSc Student
E-mail: djq@mail.sdu.edu.cn
[e]MSc Student
E-mail: 18259059558@126.com
[f]MSc Student
E-mail: 18831305237@163.com
[g]Ph.D. Student
E-mail: qyh1205@mail.sdu.edu.cn
[h]Professor
E-mail: wwenlong@sdu.edu.cn

ISSN: 2287-5301 (Print), 2287-531X (Online)

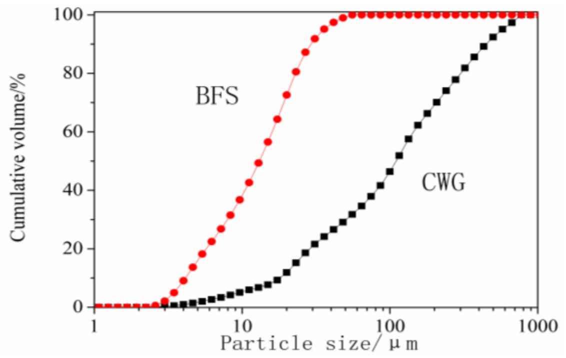

Fig. 1 Particle size distribution of raw materials

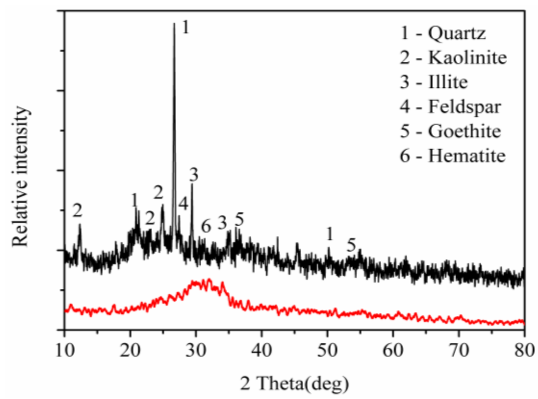

Fig. 2 XRD patterns of raw materials

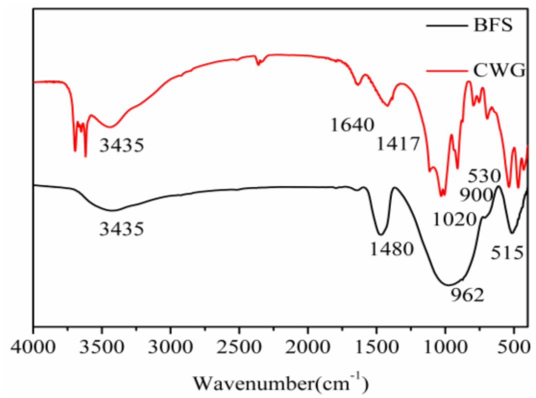

Fig. 3 IR spectra of raw materials

properties and microstructures of new geopolymer, Xiao *et al*. (2014) tested and analyzed the mechanical properties and microstructures of nickel slag based geopolymer, Wang *et al*. (2014) analyzed the mechanical properties, reaction products and microstructures of Geopolymer Materials of arsenic sandstone through X-ray diffraction, infrared spectroscopy, mercury injection, and scanning electron microscopy, and the effects of fly ash content and curing time on the mechanical properties and microstructures of geopolymer materials of arsenic sandstone were discussed. Experiments showed that the performance of geopolymer is better than that of Ordinary Portland cement. The preparation of geopolymer grouting materials from silica-alumina solid waste not only meet the engineering requirements, but also solve the environmental problems of solid waste piled up in the world.

Completely weathered granite is a kind of sandy soil with a clay content of 20-40%, and the kaolinite content of clay is appropriately 10-20% (Chiu and Ng 2014, Owie and Walton 2018). It is widely distributed in South China and is often to induce geological disasters such as water inrush and mud gush during underground engineering construction due to its easy disintegration in water and poor stability of surrounding rock (Shi *et al*. 2014, Wang *et al*. 2017). A large scale of cement slurry was used to improve the stability and mechanical property of the completely weathered granite during the construction. In this paper, a new type of geopolymeric grouting material (short for GGM) is prepared by using completely weathered granite and blast-furnace slag. GGM has the advantages of short setting time, high flowability, low viscosity, high stone rate and high compressive strength. It can be used for in-situ grouting reinforcement of completely weathered granite stratum, which can reduce the usage of cement-based grouts, and also solved the problem of waste soil during the tunnel construction, and realized the resource recycling in engineering construction.

2. Materials and experimental procedures

2.1 Raw materials

The completely weathered granite (CWG) used in the experiment came from the excavation waste soil of Junchang Tunnel in Guangxi province, China, and it was grinded to a specific surface area of 200 m^2/kg. Blast-furnace slag (BFS) was bought from Luxin Plant (Jinan, China) with a specific surface area of 400 m^2/kg. The size distribution of the two particles are shown in Fig. 1. The results of XRF (X-ray fluorescence) and XRD (X-ray diffraction) of CWG and BFS are shown in Table 1 and Fig. 2, respectively. Table 1 shows that the chemical compositions of CWG are mainly SiO_2, Al_2O_3 and a small amount of Fe_2O_3, which indicate that it has the potential to prepare geopolymer materials. The chemical compositions of BFS are mainly SiO_2, Al_2O_3 and CaO, and it has more calcium components, which could accelerate the geopolymerization process of the geopolymer. The XRD spectra shows that the main mineral compositions of CWG are quartz, kaolinite, illite, feldspar and goethite, and the BFS is mainly consists of glassy silica-alumina minerals. The IR (Infrared spectra) of CWG and BFS are shown in Fig. 3. The vibrational peak of 1020 cm^{-1} is Si-O bond, 900 cm^{-1} is Al-O bond and 530 cm^{-1} is Fe-O bond in the spectra of CWG, which indicates that there are alumino-silicate components in CWG and a certain amount of iron components. The vibration peak at 1491 cm^{-1} is Ca-O bond and that of 962 cm^{-1} is Si-O bond, which indicates that the BFS used in the experiment is alumino-silicate material. In

Table 1 Chemical composition of the raw materials

	Al_2O_3	SiO_2	CaO	Fe_2O_3+FeO	K_2O	MgO	Na_2O
CWG	27.2	49.5	0.4	5.3	0.5	5.2	0.3
BFS	12.1	23.5	57.2	0.55	0.58	2.05	0.36

Table 2 Mix design of GGM

Alkali activator concentration	Content of completely weathered granite				
	10 wt% (G1)	20 wt% (G2)	30 wt% (G3)	40 wt% (G4)	50 wt% (G5)
1.0 M (A1)	A1G1	A1G2	A1G3	A1G4	A1G5
1.5 M (A2)	A2G1	A2G2	A2G3	A2G4	A2G5
2.0 M (A3)	A3G1	A3G2	A3G3	A3G4	A3G5
2.5 M (A4)	A4G1	A4G2	A4G3	A4G4	A4G5

addition, the vibration peaks at 3453 and 3369 cm^{-1} are O-H bonds in CWG and BFS. The alkali activator of sodium hydroxide flakes with 96% purity was bought from Tianjin Dengke Chemical Reagent Co. Ltd.

2.2 Experimental procedures

In the experiment, the content of CWG were 10 wt%, 20 wt%, 30 wt%, 40 wt% and 50 wt% of the total solid raw material quality (labeled G1-G5), the concentration of alkali activator was designed as 1.0 M, 1.5 M, 2.0 M and 2.5 M (labeled A1-A4), the water to solid ratio was 1.0, which is widely used in grouting engineering. Alkali activator solution was prepared according to the designed concentration and cooled to room temperature before sample preparation. CWG, BFS and alkali activator solution were stirred uniformly according to the design ratio according to the operation of cement paste, and then poured into 40 mm×40 mm×40 mm mould to prepare samples. The samples were demoulded after 24 hours, and then maintained in water at 21°C. The curing time was 3, and 28 days (each group has 12 samples, 3 samples were tested in each curing age, and the average value was obtained.

The setting time of geopolymers was measured by Vicat test. Based on ASTM Standard C191, the initial and final setting time was recorded when the penetration height of the Vicat needle was 25 mm and less than 1 mm.

The mini-slump flow test was adopted to characterize flowability of fresh paste of geopolymer according to GB/T8077-2000 "Method for testing uniformity of concrete admixture". The viscosity evolution was conducted by SV - 10 sine wave vibration viscometer, made in Japan. The range is 0.3-10 000 mPa·s.

Vibrational bands of the specimens were determined by FTIR AVATAR 370 from Thermo Fisher Scientific Inc, Waltham, MA/ USA. The KBr pellet technique, about 1 mg powdered sample mixed with 150 mg KBr, was used for the IR test. The microstructures of geopolymer paste were investigated by scanning electron microscopy (SEM, Thermo Fisher 250 from FEI). The pore distribution was analyzed by Mercury Intrusion Porosimetry Testing (Poremaster-60, Quanta). The surface tension of mercury was set as 0.48 N/m while the contact angle was 140o. All specimens of microstructure analyzed were firstly crushed into pieces of about 3×3×3 mm at a curing age of 28-day, and stored in absolute alcohol for at least 24 h, then dried at 60°C for 24 h.

3. Results and discussion

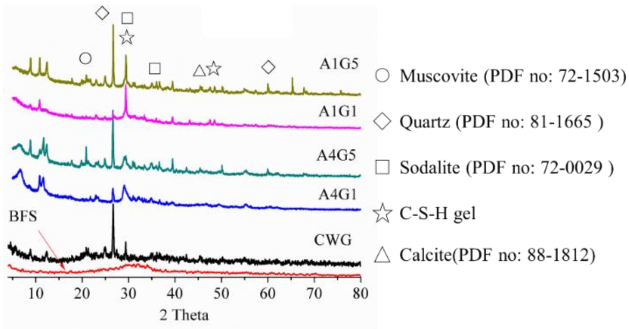

Fig. 4 XRD patterns of GGM grout under different conditions

3.1 Structural characterization of hydration products

3.1.1 XRD analysis

The hydration products of GGM grout were analyzed by X-ray diffraction. Fig. 4 shows XRD patterns of GGM grout under different conditions after cured for 28 days. It can be observed that the main hydration products of GGM are sodalite, hydrated calcium silicate, crystalline quartz, and a small amount of calcium carbonate produced by carbonation reaction of $Ca(OH)_2$ (Guo *et al*. 2016). The existence of sodium anhydrite can indirectly proves the existence of geopolymer (Bakharevt 2005), which has similar structure (same structural unit) with geopolymer. The peaks of kaolinite were disappeared in the specimen of A1G1, which presents that CWG could participate in the geopolymerization process. The peak of crystalline quartz increased as the content of CWG increased, which is due to the large amount of crystalline quartz in CWG. Muscovite was found in G5, which implied that there are a lot of unreacted CWG in the grout.

It can also be observed that, the peak of hydrated calcium silicate decreased as the concentration of alkali activator increased, as we all know that, the geopolymerization is slow down in the circumstance of lower concentration of alkali activator, and the hydrated calcium silicate has long crystallization reaction time. With the concentration of alkali activator increased, the reaction speed of geopolymerization was accelerated and the crystallization effect of hydrated products became worse. Therefore, when the concentration of alkali activator increased, the diffraction peak intensity of hydrated calcium silicate decreased.

3.1.2 IR analysis

The characteristics of chemical bonds in the hydration products were analyzed by infrared spectrum. The results of IR analysis are shown in Fig. 5. We can see that, the silicate is located in the low frequency region of 449-560 cm^{-1}, and the strong peak at 686-896 cm^{-1} is the symmetrical stretching vibration peak of Si-O-Al. The asymmetric stretching vibration peaks of Si-O-T (T=Si or Al) are observed at 968 and 1088 cm^{-1}. The vibration peak at 1450 cm^{-1} is the tensile vibration peak of O-C-O bond, which is absorbed by CO_2 during GGM polymerization. The weak vibration peaks at 1640 and 2925 cm^{-1} are the bending vibration peaks of H-O-H, which indicates that bound water

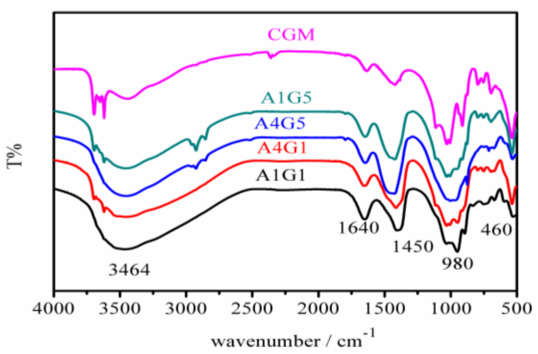

Fig. 5 IR spectrum of GGM under different conditions

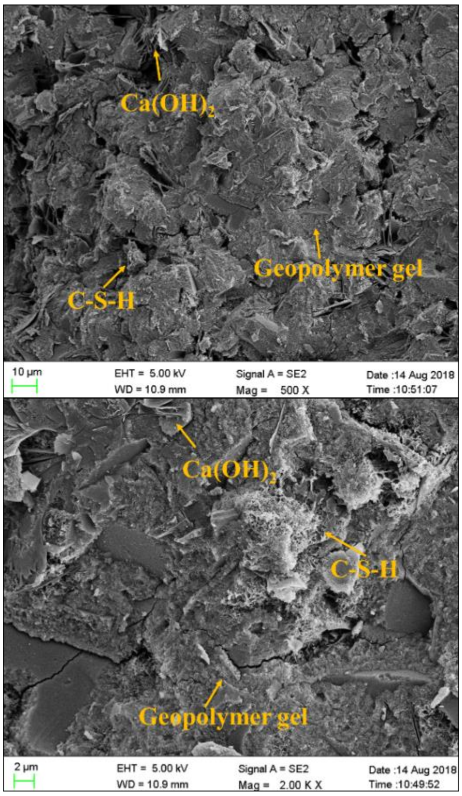

Fig. 6 SEM of GGM at 28 days

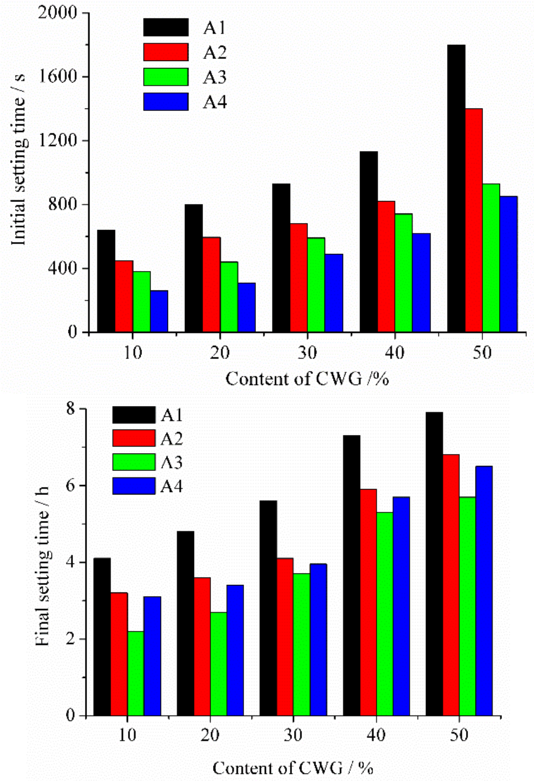

Fig. 7 Setting time of GGM with different conditions

exists in the stone body, and the broad peak at 3464cm^{-1} is the bending vibration peak of O-H, which is related to the O-H bond in the raw materials. However, these peaks are not obvious in the raw materials (Fig. 3). The change of vibration peaks of raw materials and GGM stone body and the change of the peak position of spectrum indicate that the alumino-silicate components reacted in raw materials to form geopolymer gels and hydrated calcium silicate.

It is noticeable that, the asymmetric stretching vibration peaks of Si-O-T in CWG changed significantly, which indicates that, CWG was involved in the geopolymerization process with BFS.

3.1.3 SEM analysis

The microstructure of A1G1 cured for 28 days is shown in Fig. 6. As can be seen, geopolymer gels, hydrated calcium silicate and calcium hydroxide can be found in GGM, which indicates that the alumino-silicate components in the raw materials reacted to form geopolymer. In addition, there are still unreacted CWG particles in the stone body, which provides a micro-aggregation effect on the stone body. The geopolymer gel and hydrated calcium silicate gel formed on the surface of CWG, and the particles play the role of aggregate filling.

3.2 Workability

3.2.1 Setting time

The setting time is a crucial parameter in the grouting engineering. The initial and final setting time of GGM with variable conditions are shown in Fig. 7.

It can be seen from Fig. 7 that, the initial and final setting time of GGM were prolonged as the content of CWG increased. This phenomenon illustrated that, the leached amount of Si^{4+}, Al^{3+} were lower with higher content of CWG under the same concentration of alkali activator, as the lower content of high active alumino-silicate in CWG, which delayed the polymerization process, thus prolonged the setting time of GGM.

The initial setting time of GGM decreased with the increased of alkali activator concentration, but the final setting time tended to shortened at first and then prolonged slightly. With the increased concentration of alkali activator, the leached time of Si^{4+}, Al^{3+} was shortened, the leaching amount was increased, and the polymerization reaction of geopolymer was accelerated, thus the initial setting time was shortened. When the concentration of alkali activator exceeded 10%, the concentration of alkali activator in GGM was excessive high. On the one hand, the leached time of Si^{4+}, Al^{3+} was too much that the final condensation

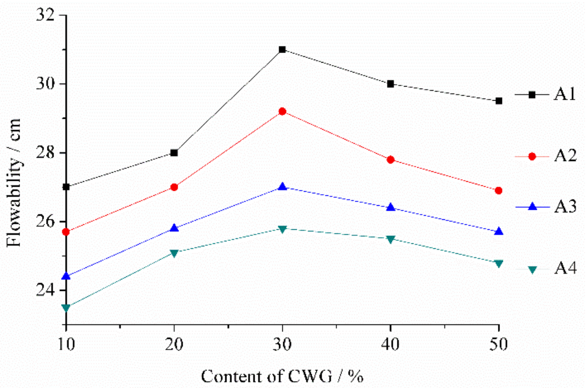

Fig. 8 Flowability of GGM with different conditions

prolonged, on the other hand, a large amount of free water and Na^+ were needed to form hydrated ions in the circumstance of high concentration of alkali activator, and the amount of free water decreased, resulted in the dissolution of SiO_4^{4-}, AlO_4^{3-} from the surface of CWG and BFS. The apparent concentration of monomers increased, and the rapid polymerization of these monomers hindered the further formation of colloids. Therefore, unlike the initial setting time, with the increased concentration of alkali activator, the final setting time tended to shortened first and then prolonged (Panias *et al*. 2007, Guo and Shi 2015).

The completely weathered granite is mostly distributed in water-rich strata. The grouting material is required to have a characteristic of short setting time in the reinforcement process. Therefore, the content of CWG and the concentration of alkali activator should be adjusted according to the actual grouting engineering requirements.

3.2.2 Flow characteristics

The flowability of grouting materials determines its pumping ability in grouting engineering. The flowability of GGM with different conditions was tested by mini-slump (Fig. 8).

As seen in Fig. 8, when the content of CWG were 10 wt%, 20 wt%, 30 wt%, 40wt% and 50 wt%, the flow diameter of fresh GGM grout (1.0 M - 2.5 M alkali activator) were 23.5-27, 25.1-28, 25.8-31, 25.5-30 and 24.8-29.5 cm, respectively. The flow diameter of GGM increased firstly and then decreased with the increased content of BFS, and decreased with the increased concentration of alkali activator. As BFS played a positive role in increasing the spreading ability due to its “filling effect” and “micro aggregate effect”. However, as the admixture percentage was up to 40 wt%, BFS has a negative effect on the flowability of grouting materials, this is because with the increased content of BFS, the specific surface area and water requirement was increased and the flowability was reduced. In addition, with the increased concentration of alkali activator, the leached time of Si^{4+} and Al^{3+} decreased and the leached amount increased, and it has an inverse ratio with the spreading ability, though the effect was weak.

As shown in Fig. 9, the time denaturation viscosity of the fresh-state GGM has low viscosity stage and solidifying stage. In the stage of low viscosity, the leaching reaction

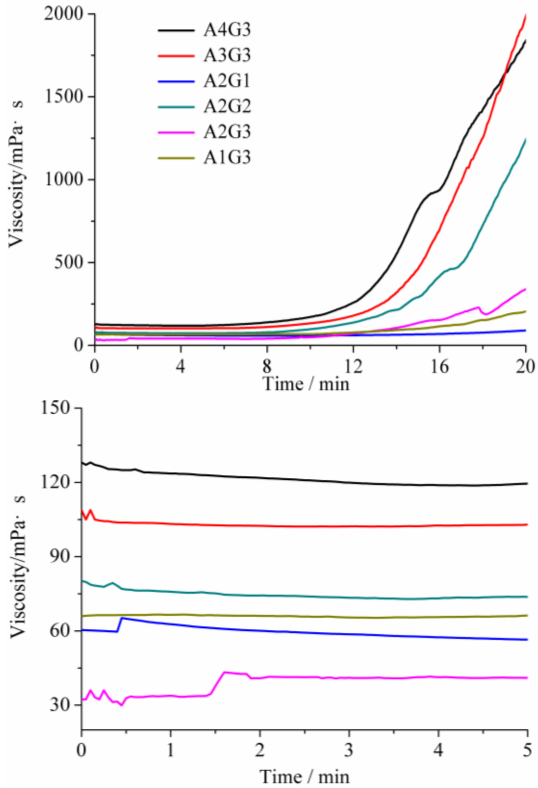

Fig. 9 Viscosity curves of GGM grout.

took place, and the viscosity stayed almost the same, as the geopolymerization process and hydration reaction began, the viscosity increased rapidly, then the solidifying stage appeared.

The viscosity has an inverse relationship with the content of CWG. This is because that, the “filling effect” and “micro-aggregate effect” of BFS played a positive role in the fresh-state GGM, and CWG particles played a negative role due to its large specific surface area .

The viscosity has a proportional relationship with the concentration of alkali activator. It is attributed to the slower leaching reaction and few amounts of Si^{4+} and Al^{3+} under the circumstance of lower alkali activator concentration. As the concentration gone up, the low viscosity stage was shorter and then the viscosity increased rapidly to the initial coagulation and continued to be thickened rapidly. At this time, GGM presented a mixture of solid and liquid, with a flow and diffusivity.

3.2.3 Stone rate

During the grouting process, the coarser particles in the slurry gradually sink, so water is forced to gradually rise to the surface of the slurry, thus affecting the stone body rate of the slurry. The treatment effect is poor in the circumstance of lower stone rate. The variation of stone rate of GGM with variable content of CWG and concentration of alkali activator are shown in Fig. 10. This paper defines the stone rate as the ratio of the volume of GGM slurry to the total volume of slurry at final setting time, and it can also be used to characterize the bleeding capacity of GGM.

It can be seen from Fig. 10 that, the stone rate of GGM showed a downward trend with the increased content of

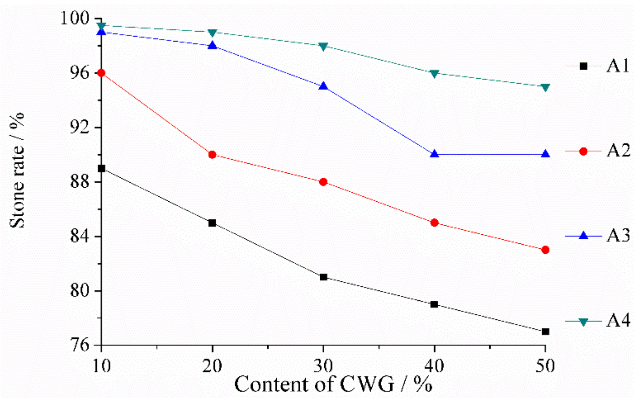

Fig. 10 Stone rate of GGM grout

CWG, which is due to the smaller particle size of BFS has higher water demand and filling effect in slurry, and the CWG has larger particle size and is easier to precipitate and segregate. In addition, the reaction activity of GGM decreased with the increased content of CWG, the setting time prolonged, the settled and segregation time of solid particles prolonged, and the stone rate of GGM decreased accordingly. Therefore, the content of CWG was inversely proportional to the stone rates.

The stone rate of GGM increased with the increased concentration of alkali activator, as the initial solidification time of GGM was shortened with the increased concentration of alkali activator, the settled and segregation time of CGM particles and BFS particles was shortened, so the stone rate of slurry increased. The leached amount of Si^{4+} and Al^{3+} increased with the increased concentration of alkali activator, the leached time shortened, and the amount of hydrogen dioxide molecules involved in polymerization increased, then a large amount of water were consolidated in the form of free water in the stone body. Therefore, with the increased of alkali activator concentration, the stone rate of GGM slurry showed an upward trend.

In the reinforcement engineering of completely weathered granite strata, the impermeability of grouting material is an important parameter to measure its durability. The impermeability of grouting material can be characterized by the pore size distribution and porosity of GGM. The pore structure characteristics of 28 d grouts stone body with different content of CWG and alkali activator concentration are shown in Figs. 11-12.

As seen in Fig. 11, the porosity and pore size of GGM increased with the increased content of CWG. This is because CWG has a larger particle size than BFS, and the activity of alumina-silicate minerals were lower than that of BFS. Under the same concentration of alkali activator, the gel content of geopolymer is very lower with a higher CWG content, so the porosity increases. It can also be seen from Fig. 11 that when the content of CWG was less than 30 wt%, its content has little effect on the porosity of GGM, because the inert mineral components in CWG played a role

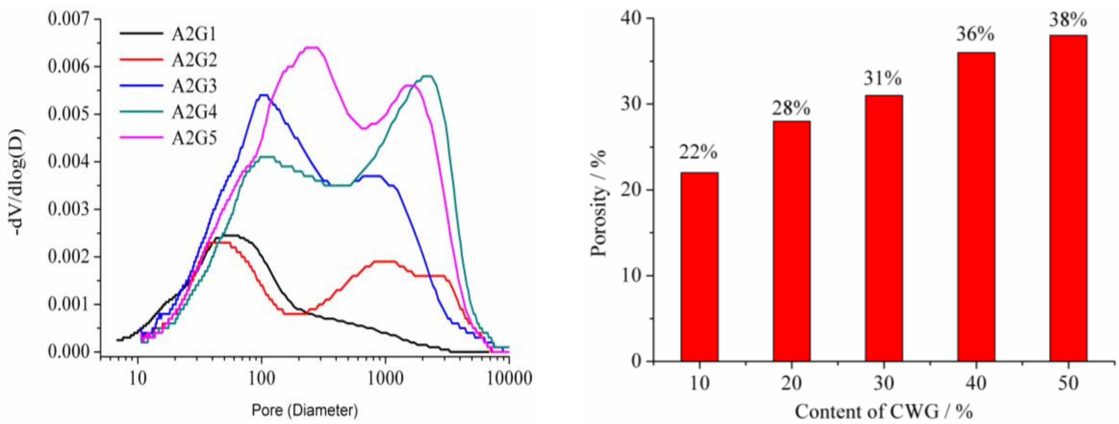

Fig. 11 MIP curves for GGM at 28 d with different content of CWG and 1.5 M alkali activator

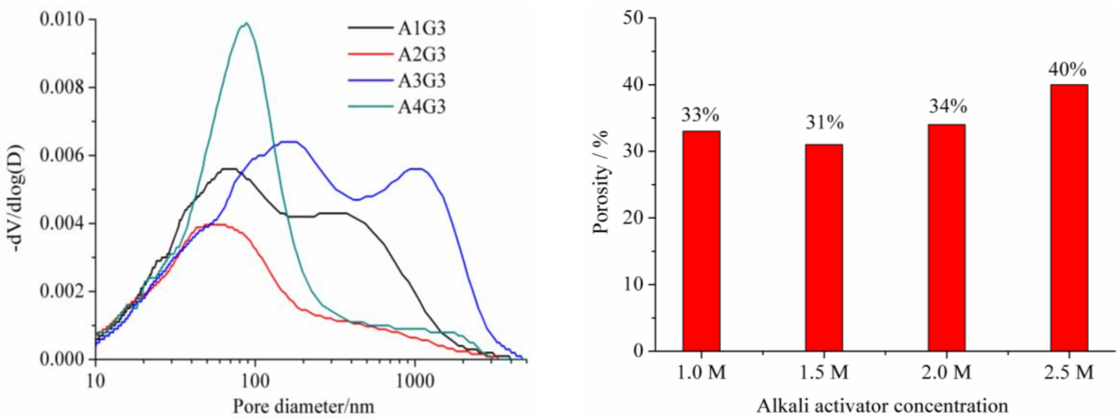

Fig. 12 MIP curves for GGM at 28 d with different alkali activator concentration and 30 wt% CWG

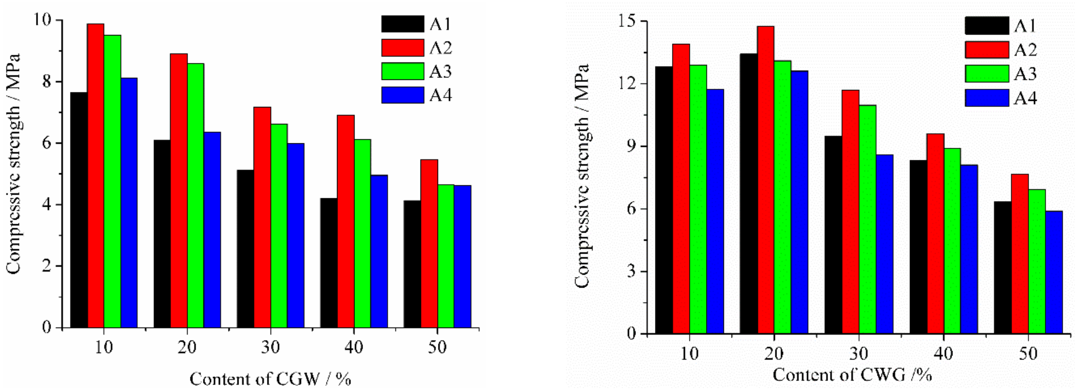

(a) 3d (b) 28d

Fig. 13 Compressive strength of GGM under different conditions

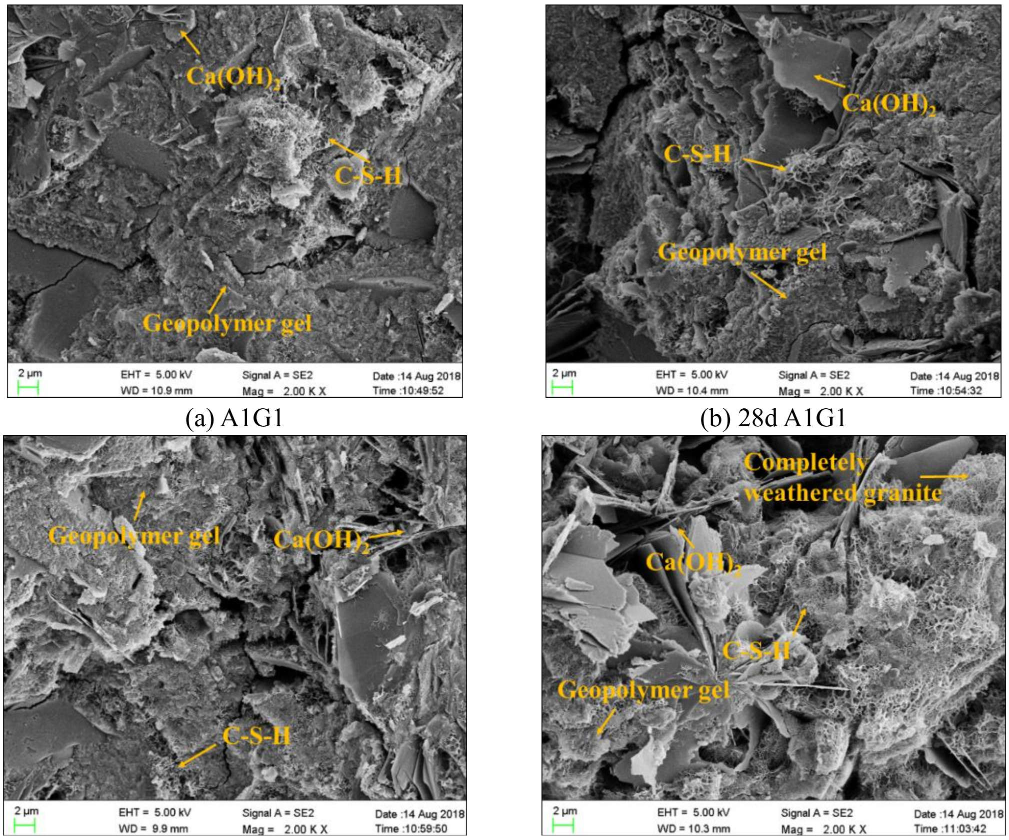

(a) A1G1 (b) 28d A1G1

(c) A1G1 (d) A1G1

Fig. 14 Compressive strength of GGM under different conditions

of aggregate.

Fig. 12 shows the pore size and porosity of GGM with different concentration of alkali activator. We can conclude that the pore size and porosity of GGM decreased first and then increased with the increasing concentration of alkali activator. With the increased concentration of alkali activator, the leached amount of Si^{4+} and Al^{3+} increased, then accelerated geopolymerization process, and the pore size and porosity decreased, but the setting time of GGM was inversely proportional to the concentration of alkali activator (Fig. 8). When the concentration of alkali activator was 10 wt%, the minimum GGM initial setting time was 5 min. With the shortened of setting time, a large amount of free water was enclosed in the stone body, which lead to the increased of the porosity. Therefore, the pore size and porosity of GGM decreased first and then increased with the increase of concentration alkali activator.

In the grouting reinforcement project of fully weathered granite strata, the porosity of consolidation body should be reduced and its impermeability should be improved so as to achieve higher grouting effect. The content of CWG should be less than 30 wt% and the concentration of alkali activator should be less than 2.0 M.

3.2.4 Compressive strength

The mechanical strength of grouting material directly affects the reinforcing ability of the material to weak stratum and the long-term stability of the injected medium. The compressive strength of GGM with different content CWG and different concentration of alkali activator concentration are shown in Fig. 13.

We can concluded from Fig. 13 that, the compressive strength of GGM increased first and then gradually decreased with the increase content of CWG. This is because the low activity of alumino-silicate mineral components in CWG, and the inert mineral components play an aggregate filling role in the process of polymerization except for some active mineral components can participate in the polymerization. With the increased content of CWG, the leaching amount of Si^{4+}, Al^{3+} of raw materials under the same concentration of alkali activator gradually decreased, and the gelled minerals of in-situ aggregates gradually decreased. Therefore, the compressive strength of GGM was inversely proportional to the content of CWG.

Comparing the compressive strength of stone body with different alkali activator concentration, it can be found that the compressive strength of GGM increased firstly and then decreased with the increased concentration of alkali activator. This is because with the increased concentration of alkali activator, the leaching ability of alumino-silicate mineral components was increased, the leaching time of Si^{4+} and Al^{3+} was shortened, and the leached amount of Si^{4+} and Al^{3+} was increased, then the polymerization reaction accelerated and the strength was enhanced. However, when the alkali concentration was beyond the optimum concentration, the apparent concentration of SiO_4^{4-}, AlO_4^{3-} monomers dissolved from the surface of CWG and BFS, which hindered the polymerization of geopolymer and reduced the compressive strength. During the hardening process of the grouts, a large amount of free water was consolidated in the stone body, which increased the pore volume of the slurry stone body and reduced its compressive strength. Therefore, the compressive strength of GGM showed a trend of first increased and then decreased with the increased concentration of alkali activator.

The microstructures of GGM (28 d) with different content CWG and different concentration of alkali activator are shown in Fig. 14.

5. Conclusions

A new geopolymeric grouting material (GGM) has been prepared by completely weathered granite (CWG) and blast-furnace slag (BFS) in this paper to solve water rush and mud gush disasters during the construction of tunnel in the completely weathered granite strata. The GGM has the advantages of short setting time, high flowability, low viscosity, high stone rate and high mechanical strength. It can be used for grouting reinforcement of completely weathered granite strata. It can not only saves a lot of cement slurry, but also solves the problem of storage waste soil. It can realizes low waste-soil emission and resource recycling in engineering construction. The following conclusions were drawn:

- Completely weathered granite can participates in the geopolymerization process with blast-furnace slag, what's more, it has a micro-aggregation effect on the GGM.
- The setting time of GGM grouting material were 5-30 minutes, the flowability was more than 23.5 cm, the stone rate is higher than 93%, the compressive strength of GGM could be adjust in the range of 7.8-16.9 MPa in 28 d, and the porosity was lower than 34% by adjusting the content of CWG and the concentration of alkali activator,. In order to meet the requirement of grouting reinforcement for completely weathered granite strata, the content of CWG should be less than 30 wt%, and the concentration of alkali activator should be 1.0-2.0 M.
- Microstructure analysis showed that the main reaction products of GGM were geopolymer gel, hydrated calcium silicate gel (C-S-H), calcium hydroxide and calcium carbonate. With the increased content of CGM, the porosity of stone body gradually increased. The porosity of stone body first decreased and then increased with the increased concentration of alkali activator.

Acknowledgments

This study was financially supported by the Major basic Project of Shandong Provincial Natural Science Foundation of China (Project Nos. ZR2017ZC0734), the Major Project of Chinese National Programs for Fundamental Research and Development (Project No. 2017YFC0703100), the Young Scientists Funds of National Natural Science Foundation of China (Grants Nos. 51709158), the China Postdoctoral Science Foundation Funded Project (No. 2018M632676).

References

Bakharev, T. (2005), "Durability of geopolymer materials in sodium and magnesium sulfate solutions", *Cement Concrete Res.*, **35**(6), 1233-1246. https://doi.org/10.1016/j.cemconres.2004.09.002.

Chen, C., Habert, G., Bouzidi, Y. and Jullien, A. (2010), "Environmental impact of cement production: detail of the different processes and cement plant variability evaluation", *Clean. Prod.*, **18**(5), 478-485. https://doi.org/10.1016/j.jclepro.2009.12.014.

Chiu, C.F. and Ng, C.W. (2014), "Relationships between chemical weathering indices and physical and mechanical properties of decomposed granite", *Eng. Geol.*, **179**(10), 76-89. https://doi.org/10.1016/j.enggeo.2014.06.021.

Davidovits, J. (1991), "Geopolym", *J. Therm. Anal. Calorim.*, **37**, 1633-1656.

Duan, P., Yan, C., Zhou, W. and Ren, D. (2016), "Fresh properties, compressive strength and microstructure of fly ash geopolymer paste blended with iron ore tailing under thermal cycle", *Constr. Build. Mater.*, **118**, 76-88. https://doi.org/10.1016/j.conbuildmat.2016.05.059.

Duxson, P., Fernández-Jiménez, A., Provis, J.L., Lukey, G.C., Palomo, A. and van Deventer, J.S. (2007), "Geopolymer technology: the current state of the art", *J. Mater. Sci.*, **42**, 2917-2933. https://doi.org/10.1007/s10853-006-0637-z.

El-Naggar, M.R. and El-Dessouky, M.I. (2017), "Re-use of waste glass in improving properties of metakaolin-based geopolymers: Mechanical and microstructure examinations", *Constr. Build. Mater.*, **132**, 543-555. https://doi.org/10.1016/j.conbuildmat.2016.12.023.

Guo, X. and Shi, H. (2015), "Metakaolin-, fly ash- and calcium hydroxide-based geopolymers: effects of calcium on performance", *Adv. Cement Res.*, **27**(10), 559-566. https://doi.org/10.1680/jadcr.14.00081.

Guo, X., Shi, H. and Hu, W. (2016), "Setting time and rheological properties of solid waste-based composite geopolymers", *J. Tongji Univ. (Nat. Sci.)*, **44**(7), 1066-1071.

Hong, K. (2017), "Typical underwater tunnels in the mainland of China and related tunneling", *Technol. Eng.*, **3**(6), 871-879. https://doi.org/10.1016/j.eng.2017.12.007.

Jindal, B.B., Singhal, D., Sharma, S.K. and Ashish, D.K. (2017), "Improving compressive strength of low calcium fly ash geopolymer concrete with alccofine", *Adv. Concrete Constr.*, **5**(1), 17-29. https://doi.org/10.12989/acc.2017.19.2.017.

Kurtoglu, A.E., Alzeebaree, R., Aljumaili, O., Nis, A., Gulsan, M.E., Humur, G. and Cevik, A. (2018), "Mechanical and durability properties of fly ash and slag based geopolymer concrete", *Adv. Concrete Constr.*, **6**(4), 365-362. https://doi.org/10.12989/acc.2018.6.4.345.

Li, C., Zhang, T. and Wang, L. (2014), "Mechanical properties and microstructure of alkali activated Pisha sandstone geopolymer composites", *Constr. Build. Mater.*, **68**, 233-239. https://doi.org/10.1016/j.conbuildmat.2014.06.051.

Li, S., Liu, R., Zhang, Q. and Zhang, X. (2016), "Protection against water or mud inrush in tunnels by grouting", *J. Rock Mech. Geotech. Eng.*, **8**(5), 753-766. https://doi.org/10.1016/j.jrmge.2016.05.002.

Mehta, A. and Siddique, R. (2016), "An overview of geopolymers derived from industrial by-products", *Constr. Build. Mater.*, **127**, 183-198. https://doi.org/10.1016/j.conbuildmat.2016.09.136.

Ng, C., Alengaram, U.J., Wong, L.S., Mo, K.H., Jumaat, M.Z. and Ramesh, S. (2018), "A review on microstructural study and compressive strength of geopolymer mortar, paste and concrete", *Constr. Build. Mater.*, **186**, 550-576. https://doi.org/10.1016/j.conbuildmat.2018.07.075.

Owie, S. and Walton, G. (2018), "The effect of mineralogical parameters on the mechanical properties of granitic rocks", *Eng. Geol.*, **5**(24), 204-225. https://doi.org/10.1016/j.enggeo.2018.04.021.

Panias, D., Giannopoulou, I.P. and Perraki, T. (2007), "Effect of synthesis parameters on the mechanical properties of fly ash-based geopolymers", *Coll. Surf. A: Physicochem. Eng. Aspect.*, **301**(1-3), 246-254. https://doi.org/10.1016/j.colsurfa.2006.12.064.

Puertas, F., Fernández-Jiménez, A. and Blanco-Varela, M.T. (2004), "Blanco-Varela MT. Pore solution in alkali activated slag cement pastes. Relation to the composition and structure of calcium silicate hydrate", *Cement Concrete Res.*, **34**, 139-148. https://doi.org/10.1016/S0008-8846(03)00254-0.

Schneider, M., Romer, M., Tschudin, M. and Bolio, H. (2011), "Sustainable cement production-present and future", *Cement Concrete Res.*, **41**(7), 642-650. https://doi.org/10.1016/j.cemconres.2011.03.019.

Shi, Y., Yang, J. and Wang, S. (2014), "Sub-horizontal reinforcement of weathered granite before tunneling beneath a spillway", *Int. J. Rock Mech. Min. Sci.*, **72**(72), 283-293. https://doi.org/10.1016/j.ijrmms.2014.08.005.

Tchadjie, L.N. and Ekolu, S.O. (2018), "Enhancing the reactivity of aluminosilicate materials toward geopolymer synthesis", *J. Mater. Sci.*, **53**, 4709-4733. https://doi.org/10.1007/s10853-017-1907-7.

Wang, K., Li, S., Yang, L., Zhang, Q., Li, Z. and Yuan, J. (2017), "Grouting simulation experiment on reinforcement characteristics of completely decomposed granite", *J. Tianjin Univ. (Sci. Technol.)*, **50**(11), 1199-1209.

Yang, T., Yao, X. and Zhang, Z. (2014), "Geopolymer prepared with high-magnesium nickel slag: Characterization of properties and microstructure", *Constr. Build. Mater.*, **59**, 188-194. https://doi.org/10.1016/j.conbuildmat.2014.01.038.

Zhang, Y.C. (2012), *Cementation Technology*, Coal Industry publishing House, Beijing, CHINA.

CC